Journal of Engineering Physics and Thermophysics, Vol. 77, No. 4, 2004

EFFECT OF A ROTATING MAGNETIC FIELD ON CONVECTION STABILITY AND CRYSTAL GROWTH IN ZERO GRAVITY AND ON THE GROUND

A. I. Feonychev and N. V. Bondareva

UDC 538.4:532.6:532.78

A numerical study of the flows arising in a conducting liquid under the action of a rotating magnetic field as well as under its interaction with gravitational and thermocapillary convection has been made. The boundaries of the transition to the oscillating regime of convective flows have been determined. Regions of mixed flows, in which the impurity macrosegregation in crystals grown by the Bridgman and floating-zone methods decrease, have been revealed. It has been shown that regions of flows in which both a smooth increase in the impurity macrosegregation and a change in the form of a clearly defined extremum are observed also exist. The possibilities of mathematical modeling of geophysical problems with the use of a rotating magnetic field are discussed.

Introduction. With increasing number of elements in large-scale integration circuits, the general tendency being towards microminiaturization of electronic systems, the requirements on micro- and macrohomogeneity of monocrystals are becoming more stringent. To control the transfer of doping impurities in the process of monocrystal growth, various methods are used: rotation, vibration, acoustic and magnetic fields. At present, further improvement of the methods for growing monocrystals is only possible with a detailed study of the melt flow and the heat-and-mass transfer under these conditions. The methods of mathematical modeling thereby play the determining role, since they permit finding the direction of further experimental studies and estimating the expected effect of proposed improvements. In the last few years, more and more attention has been given to the effects of a rotating magnetic field (RMF) during growth of monocrystals of semiconductor materials from melts having in the liquid state electrical conduction in metals.

An RMF is applied during continuous casting of steel to intensify the stirring of the liquid metals with the aim of obtaining a better structure of the alloy and decreasing the porosity and liquation inhomogeneity of ingots. The investigation of the magnetohydrodynamic flows as applied to this technology was conducted using approximate mathematical models and calculation algorithms. This is due to the fact that the problem solution is a complicated task of computational mathematics. In the three-dimensional flow generated by the RMF, the determining role is played by the secondary flow arising in a limited volume of rotating liquid. To determine the secondary-flow components, the authors of [1, 2] used integral relations, and the authors of [3] used the method of expansion in the small parameter, the Ekman number, characterizing the viscous boundary-layer thickness at the end surfaces of a liquid cylindrical space. To describe the turbulent flow of the melt in a real technological process, turbulence models obtained for the condition of external flow over solid surfaces were used. In [4, 5], of greatest interest are the experimental data.

The rotating magnetic field began to be used in the technology of single-crystal growing relatively recently. In so doing, different methods of single-crystal growth were considered: the Czochralskii and Bridgman methods [6] and the moving-heater [7–9] and floating-zone [10] methods. In [6, 10], the crystal growth was influenced by the earth's gravitational acceleration, in [7, 8] — by a lowered gravitational acceleration ($g = 10^{-3}$ of earth's acceleration), and, finally, in [9] — an acceleration close to zero ($g \sim 10^{-5}$ of earth's acceleration). In the Bridgman and moving-heater methods, the liquid is confined within the solid ends and the solid side walls of the ampoule. In the Czochralskii and floating-zone methods, the liquid has free surfaces and the flow in the rotating liquid interacts with the

Moscow Aircraft Institute, 5 Leningradskoye Shosse, Moscow, 125080, Russia; email: ab246@mail.sitek.ru.
Translated from Inzhenerno-Fizicheskii Zhurnal, Vol. 77, No. 4, pp. 50–61, July–August, 2004. Original article submitted April 30, 2003; revision submitted September 3, 2003.

1062-0125/04/7704-0731

thermocapillary convection caused by the temperature dependence of the surface tension. The melt flow rates during crystal growth are much lower, which simplifies the development of programs for exact numerical investigations of these processes.

In [6–8], primary consideration was given to the RMF dependence of the form of the crystallization boundary. These studies have shown that the influence of the RMF on the form of the interphase boundary is weak and indefinitive [6, 7]. In the experiment performed on board the Photon-7 and Photon-9 drone space vehicles [9], only a positive effect connected with the obtaining of a more uniform impurity distribution along the crystal axes with the use of a rotating magnetic field was noted. This effect could be predicted on the basis of the available data on the impurity distribution in carrying out the technological process in zero gravity and the slow flows generated in the liquid by a rotating low-intensity magnetic field ($Ha^2Re_\omega = 3.3\cdot10^3–7.6\cdot10^5$) in microgravity. The same data permit concluding that the secondary flow generated by a relatively weak RMF should lead to an increase in the radial nonuniformity (impurity microsegregation). Moreover, the subsequent analysis has shown [11] that individual flow conditions fall within the region of the maximum of the radial impurity distribution nonuniformity.

In the experiment on crystal growth by the floating-zone method performed on the ground [10], a decrease in the temperature oscillation and impurity banding (impurity microsegregation) in the silicon crystal obtained with the use of an RMF was observed. Such an effect of a rotating magnetic field could be expected. It is known that the appearance of a weak azimuthal velocity leads to oscillation thermocapillary convection. A strong rotating liquid flow generated by a magnetic field should lead to an averaging of the azimuthal velocity and an increase in the three-dimensional flow stability. In one of the figures in [10], some increase in the radial macrononuniformity of the impurity distribution (radial impurity macrosegregation) can be noted. However, this effect is not discussed in the publication. We also note that [10] presents a preliminary ground investigation, which should be completed with an experiment in microgravity. Thus, it can be noted that the problem of optimization of the RMF parameters in the process of single-crystal growth is topical.

Numerical investigations make it possible to choose a correct direction of experimental studies and considerably promote this work and reduce its cost, which is particularly important for space material science. Technological processes of crystal growth are much slower than the process of continuous casting of steel. Therefore, one can use the well-developed methods of numerical studies of viscous incompressible liquid flows and heat-and-mass transfer.

We began to study the problem of using the RMF with systematic numerical calculations of the flow structure at boundary conditions corresponding to different methods of crystal growth. We considered regimes with a combination of the secondary flow generated by the RMF with the thermal gravitational or thermocapillary convection in [12]. To increase the accuracy of calculations in the region of higher liquid flow rates, including the oscillating regime, we developed programs for numerical solution of the Navier–Stokes equations with a higher order of approximation by spatial coordinates. On the basis of the works devoted to numerical investigations of the problem of crystal growth by different methods [13–15], the direction of the investigation that can give a positive effect in using the RMF was determined. First, it is necessary to determine the boundary of the transition to the oscillating regime of convection in order to exclude temperature oscillations and impurity segregation. Second, it is necessary to investigate the dependence of the radial impurity macrosegregation on the RMF parameters and find those parameters of the magnetic field that can provide a decrease in the radial impurity macrosegregation. Thus, the problem of optimizing the RMF parameters in the process of single-crystal growth in microgravity is stated.

1. Problem Formulation and Solution Method. Consider a liquid flow in a cylindrical space of radius R and length L, on which an external rotating magnetic field is acting. The latter is generated by coils located around the liquid cylinder, and the axes are directed along the radius. The coil windings are energized by alternate current so that the pole pairs lie on one diameter. When alternate current with a cyclic frequency ω is supplied, the magnetic field generated by the coils rotates about the cylinder axis. Write the magnetic induction components along the radius r and in azimuthal angle φ in the form [2, 4]

$$B_r = B\sin(\omega t)\,, \quad B_\varphi = B\cos(\omega t)\,. \tag{1}$$

The gaps between the electromagnet poles and the liquid are minimal. It is assumed that the length of the magnetic field zone is larger than the liquid length and the magnetic induction modulus is constant with r and the z

axis. The liquid-zone ends (growing and melting crystals) have a conduction close to that of the liquid zone. The induced electric current is closed through the ends in the external circuit. The side surface of the liquid is a solid wall from a dielectric material (it is most commonly a quartz ampoule wall) or a free surface contacting vacuum or a nonconducting gas.

The inductionless approximation is used [16], since the magnetic Reynolds number $\mathrm{Re_m} = \mu_0 \lambda R V_{\max} << 1$, where $V_{\max}$ is the characteristic (maximum) velocity. This condition is fulfilled for all regimes under investigation.

The distribution of currents and fields in a flowing conducting liquid in the general case can be found from the system of Maxwell equations and the Ohm law written in the vector form

$$\mathrm{rot}\,\mathbf{E} = -\partial\mathbf{B}/\partial t\,, \quad \mathrm{div}\,\mathbf{j} = 0\,, \quad \mathbf{j} = \lambda\,(\mathbf{E} + \mathbf{V}\times\mathbf{B})\,, \tag{2}$$

with the boundary conditions

$$r = R\,, \quad E_r = 0\,; \quad z = 0\,, \quad z = L\,, \quad E_r = E_\varphi = 0\,; \quad r = 0\,, \quad \text{symmetry condition}. \tag{3}$$

Further simplification of Eqs. (2) is connected with the fact that, according to the problem conditions, convective electric currents, as compared to conduction currents, can be neglected. The magnetic field rotation frequency is small (less than a few kilohertz). The difference in electrical conduction between the liquid and solid ends is also small. Therefore, in both media the skin-layers are thick, and the electrovortex flow arising from the conduction jump at the liquid–solid interface is negligibly small. Thus, for the electric field we have the approximate equations

$$\mathrm{rot}\,\mathbf{E} = -\partial\mathbf{B}/\partial t\,, \quad \mathrm{div}\,\mathbf{E} = 0\,. \tag{4}$$

Using Eqs. (1), (3), and (4) for the projections of the electric field strength, we obtain the following expressions:

$$E_r = E_\varphi = 0\,, \quad E_z = r\omega B_r = r\omega B\sin(\omega t)\,. \tag{5}$$

Now we can determine the projections of the Lorentz force created by the RMF:

$$F_r = -\lambda u B_\varphi^2 - \lambda B_r B_\varphi \omega r\,(1 - w/\omega r)\,, \quad F_\varphi = \lambda B_r^2 \omega r\,(1 - w/\omega r) + \lambda B_r B_\varphi\,, \quad F_z = -\lambda B^2 v\,. \tag{6}$$

Below we will consider an axially symmetric flow. Therefore, upon averaging over the rotation frequency, we obtain for such a flow Lorentz force projections in the form

$$F_r = -\frac{1}{2}\lambda B^2 u\,, \quad F_\varphi = \frac{1}{2}\lambda B^2 \omega r\,(1 - w/\omega r)\,, \quad F_z = -\frac{1}{2}\lambda B^2 v\,. \tag{7}$$

The liquid flow in a cylindrical space under the action of gravitational acceleration along the axis is described by the following system of dimensionless equations for a viscous incompressible liquid:

$$\frac{\partial u}{\partial r} + \frac{u}{r} + \frac{\partial v}{\partial z} = 0,$$

$$\frac{\partial u}{\partial \tau} + u\frac{\partial u}{\partial r} + v\frac{\partial u}{\partial z} - \frac{w^2}{r} = -\frac{\partial p}{\partial r} + \left(\frac{1}{r}\frac{\partial u}{\partial r} + \frac{\partial^2 u}{\partial r^2} + \frac{\partial^2 u}{\partial z^2} - \frac{u}{r^2}\right) - \mathrm{Gr}\frac{\partial \theta}{\partial r} - \frac{u}{2}\mathrm{Ha}^2,$$

$$\frac{\partial v}{\partial \tau} + u\frac{\partial v}{\partial r} + v\frac{\partial v}{\partial z} = -\frac{\partial p}{\partial z} + \left(\frac{1}{r}\frac{\partial v}{\partial r} + \frac{\partial^2 v}{\partial r^2} + \frac{\partial^2 v}{\partial z^2}\right) - \frac{v}{2}\mathrm{Ha}^2,$$

$$\frac{\partial w}{\partial \tau} + u\frac{\partial w}{\partial r} + w\frac{u}{r} = \left(\frac{1}{r}\frac{\partial w}{\partial r} + \frac{\partial^2 w}{\partial r^2} + \frac{\partial^2 w}{\partial z^2}\right) + \frac{1}{2}\mathrm{Ha}^2\,\mathrm{Re}_\omega\left(1 - \frac{w}{\mathrm{Re}_\omega}\right), \tag{8}$$

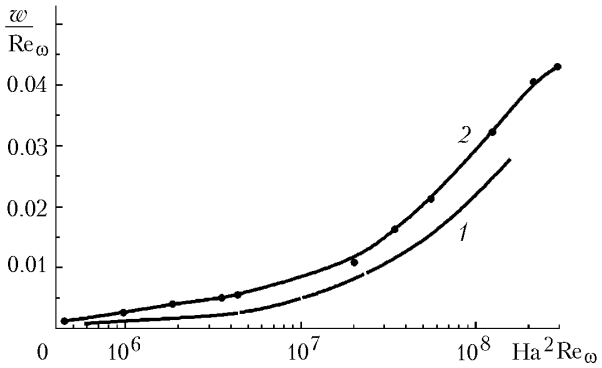

Fig. 1. Comparison of the calculations with the experimental data of [2]: 1) calculation; 2) experiment. $\mathrm{Re}_\omega = 2.46 \cdot 10^6$, Ha is variable.

$$\frac{\partial \theta}{\partial \tau} + u\frac{\partial \theta}{\partial r} + v\frac{\partial \theta}{\partial z} = \mathrm{Pr}^{-1}\left(\frac{1}{r}\frac{\partial \theta}{\partial r} + \frac{\partial^2 \theta}{\partial r^2} + \frac{\partial^2 \theta}{\partial z^2}\right),$$

$$\frac{\partial C}{\partial \tau} + u\frac{\partial C}{\partial r} + v\frac{\partial C}{\partial z} = \mathrm{Sc}^{-1}\left(\frac{1}{r}\frac{\partial C}{\partial r} + \frac{\partial^2 C}{\partial r^2} + \frac{\partial^2 C}{\partial z^2}\right).$$

In deriving these equations, the Joule heat was neglected. We used the following scales for the linear size, velocity, time, pressure, impurity concentration, and magnetic induction: R, vR^{-1}, $R^2\nu^{-1}$, $\rho\nu^2R^{-2}$, c_0, and B.

Note that the parameters $\mathrm{Ha}^2\mathrm{Re}_\omega$ and Ha determine the influence of the RMF on the liquid flow. The complex parameter $\mathrm{Ha}^2\mathrm{Re}_\omega$ thereby creates a rotational flow of the liquid in the fourth equation of (8), and the Hartmann number acts on the flow as does the steady-state magnetic field, i.e., it retards the flow.

At the crystallization boundary ($z = 0$) the doping impurity either precipitates or is absorbed, depending on the value of the coefficient k: the impurity precipitates into the melt if $k < 1$ and is absorbed if $k > 1$. The impurity flow was calculated by the relation obtained in [11], which takes into account the mass balance of impurity in the liquid and in the melt in the process of crystals growth:

$$-(\partial C/\partial z)_s = \mathrm{Re}_{cr}\mathrm{Sc}\,(1 - kC_s)\,. \tag{9}$$

The thermal boundary conditions depend on the method of crystal growth. For the Bridgman method on the side surface the parabolic temperature distribution $\theta = (z/L)^{1/2}$ from the zero value at the crystallization boundary ($z = 0$) to $\theta = 1$ at $z = L$ was given. If the floating-zone method is considered, then on the free side surface the distribution of the heat flow supplied to the liquid zone from the outside is given in the form of the exponent

$$\frac{\partial \theta}{\partial r} = a\exp\left[-b\left(z - \frac{L}{2}\right)^2\right], \tag{10}$$

and at the boundary $z = 0$ and $z = L$ (melting and crystallization boundaries) always $\theta = 0$, i.e., symmetry of thermal conditions about the plane $z = L/2$ exists.

All velocity components at solid boundaries are equal to zero, and on the free side surface of the liquid $r = 1$ in the floating-zone method a kinematic condition for the thermocapillary effect takes place to create in the liquid the thermocapillary convection

$$\frac{\partial v}{\partial r} = -\,\mathrm{Ma}\,\mathrm{Pr}^{-1}\left(\frac{\partial \theta}{\partial z}\right). \tag{11}$$

For the numerical solution of the pseudo-three-dimensional (there is no dependence of parameters on the azimuthal coordinate φ) system of equations (8), a finite-difference implicit scheme with a higher, third order of accu-

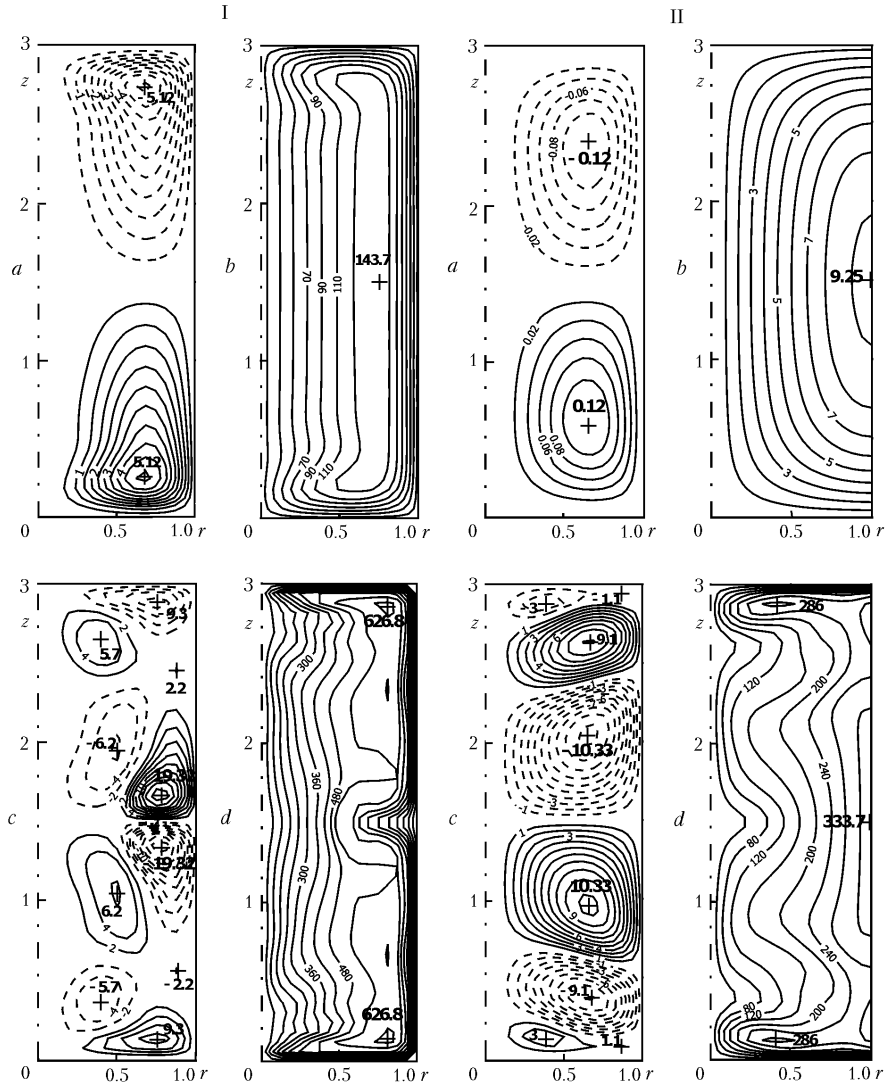

Fig. 2. Structure of the flow (stream function fields (a, c)) and circular velocity distributions (b, d) in the liquid (Pr = 0.018) completely filling a cylindrical vessel — I (Ha = 1, $Re_\omega = 10^4$ (a, b); Ha = 2, $Re_\omega = 2 \cdot 10^4$ (c, d)), and a vessel with a free cylindrical surface — II (Ha = 1, $Re_\omega = 10^2$ (a, b); Ha = 0.5, $Re_\omega = 4 \cdot 10^4$ (c, d)).

racy in spatial coordinates is used. The scheme permits one to obtain a stable solution up to flow velocities conforming to the oscillating regime of convection. An effective computational algorithm permitting calculations with large time steps is used. This difference scheme was used by us in a number of works [11–15].

2. Results of the Calculations. The mathematical model used to investigate the effects of the RMF was tested (Fig. 1) by comparison with the results of experiments with mercury filling a cylindrical vessel (Pr = 0.023) [2]. The ratio of the maximum value of the azimuthal velocity to the rotational velocity of the magnetic field increases with increasing magnetic field intensity in the experiment as it does in the calculation. The quantitative difference can be attributed to the fact that in the experiment the rotational velocity of the liquid was measured by a propeller placed in the liquid. Such a device gives a velocity value not on one axis of the spatial flow but a certain combination of three velocity components.

2.1. Determination of the boundary of the transition from the laminar-flow conditions to the oscillating regime of convection. For better understanding of the interaction between the flow generated by the RMF and the flow arising by another mechanism, we show the flow structure (current function ψ and dimensionless azimuthal velocity W fields)

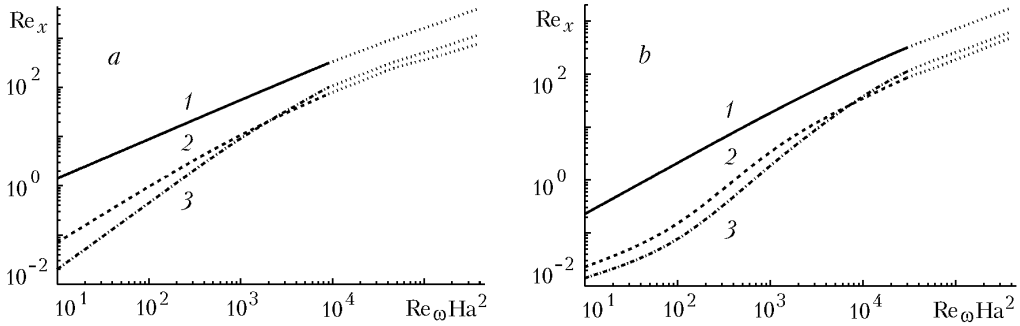

Fig. 3. Characteristic velocities versus the rotating magnetic field intensity for a liquid with a solid (a) and a free (b) side surface: 1) W_{max}; 2) V_{max}; 3) U_{max}. L/R = 3, Ha = 1 (Ge (Ga)).

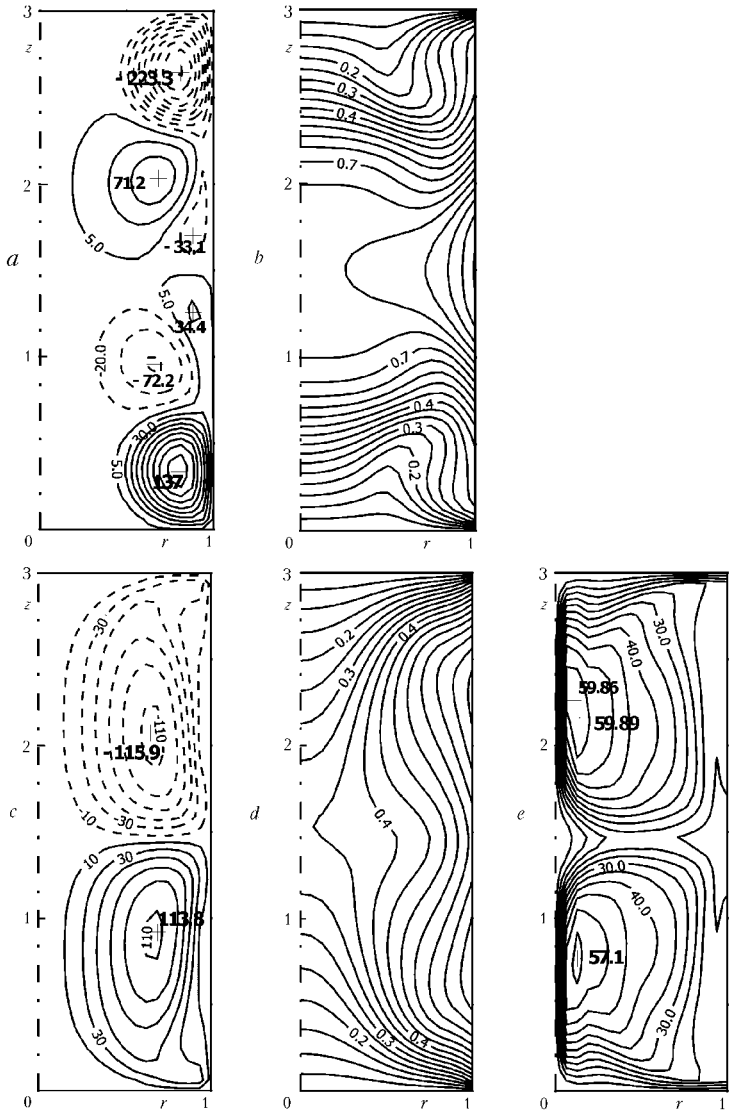

Fig. 4. Structure of the flow (stream function fields (a, c)), temperature fields (b, d), and circular velocity distribution (e) in the liquid (Pr = 0.018) for thermocapillary convection without a magnetic field (a, b) and with a magnetic field (c, d, e). Ma = 2430, Ha = 2, $Re_\omega = 1 \cdot 10^3$.

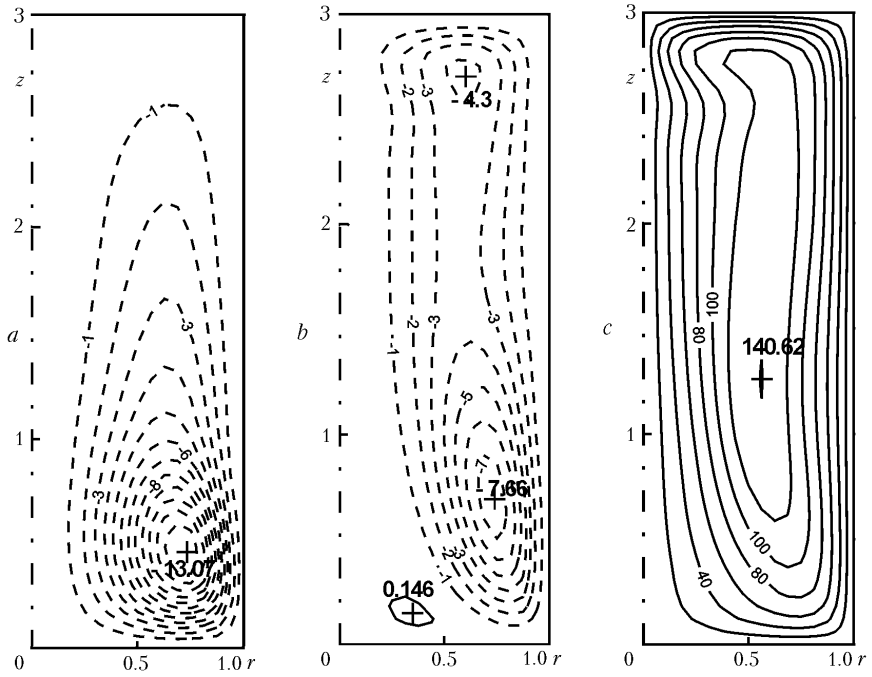

Fig. 5. Structure of the flow (stream function fields (a, b)) and circular velocity distribution (c) in the liquid (Pr = 0.023) for gravitational thermal convection without a magnetic field (a) and with a magnetic field (b, c). Gr = $4 \cdot 10^5$, Ha = 0.158, $\mathrm{Re}_\omega = 2.5 \cdot 10^5$.

in a cylindrical space with a solid surface (Fig. 2, I) and a free side surface (Fig. 2, II). Here, as in all of the following figures, solid lines of current correspond to a clockwise flow and dashed lines indicate a counterclockwise flow. In the rotating liquid, under the action of the centrifugal force there arises a flow from the rotation axis to the periphery and a return flow at the solid ends where the liquid is retarded due to the viscous friction. Viscous Ekman layers in the liquid arise not only at the ends but also on the side solid surface (Fig. 2, I). The upper row (a, b) shows the case of a flow under laminar conditions, and the lower row (c, d) — the spontaneous structure in the oscillating flow regime. Note that the azimuthal velocity gradient dramatically increases at the solid ends with increasing rotation velocity of the liquid in both cases. It is here that the flow stability is lost and oscillations arise. Note that the azimuthal velocity has a maximum value on the free surface only under the laminar-flow conditions (Fig. 2, IIb). In the other cases, the azimuthal velocity maximum is positioned in the vicinity of the solid ends.

The dependence of the characteristic flow velocities (maximum values of the azimuthal velocity $W_{\max}$ and secondary flow components $U_{\max}$, $V_{\max}$) on the complex parameter $\mathrm{Ha}^2\mathrm{Re}_\omega$ characterizing the rotating magnetic field intensity is given in Fig. 3. Note first that the secondary flow intensity is very high and this flow can only be neglected if $\mathrm{Ha}^2\mathrm{Re}_\omega < 10^2$. Second, the changeover to the oscillating regime of flow (beyond this boundary the curves in Fig. 3 are shown by dots) occurs at $W_{\max} = 300$ in both cases. The azimuthal velocity gradients at the ends at the instant of onset of oscillations are also approximately equal. The $\mathrm{Ha}^2\mathrm{Re}_\omega$ parameter at the transition boundary is equal to $9.5 \cdot 10^3$ for the case of the free side surface and $3 \cdot 10^4$ for the solid surface.

Figure 4 gives the stream function, temperature, and azimuthal velocity fields for pure thermocapillary convection (upper row) and thermocapillary convection in combination with an RMF (lower row). The thermal boundary condition in this case corresponds to crystal growth by the floating-zone method, i.e., the thermal flow distribution at the boundary $r = 1$ according to relation (10) is given. The thermocapillary convection at Ma = 2430 is oscillatory and Fig. 4a and b shows the instantaneous fields of the parameters. Oscillations cease and the flow becomes stationary when an RMF is applied (Fig. 4c–e). The flow generated by the RMF in the plane (r, z) is close in structure to the thermocapillary flow, and their interaction leads to a change in the velocity gradients near the region boundaries. At interaction of the RMF with gravitational convection a combination of flows widely differing in structure occurs, which is clearly seen from Fig. 5.

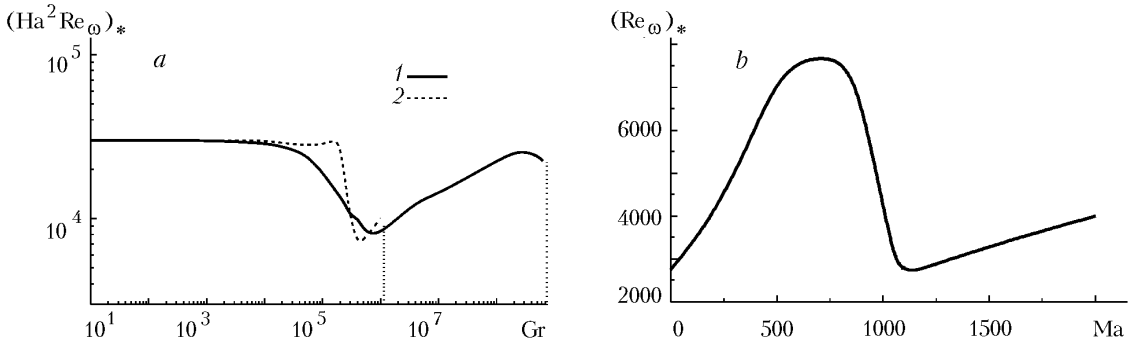

Fig. 6. Stability boundary of thermal gravitational (a) and thermocapillary (b) convection with a rotating magnetic field: 1) toward the crystallization boundary; 2) from the crystallization boundary. Ha = 0.158, L/R = 3, a = 0.47735, b = 0.5 (a); Ha = 4, L/R = 2, a = 0.8, b = 0.3 (b).

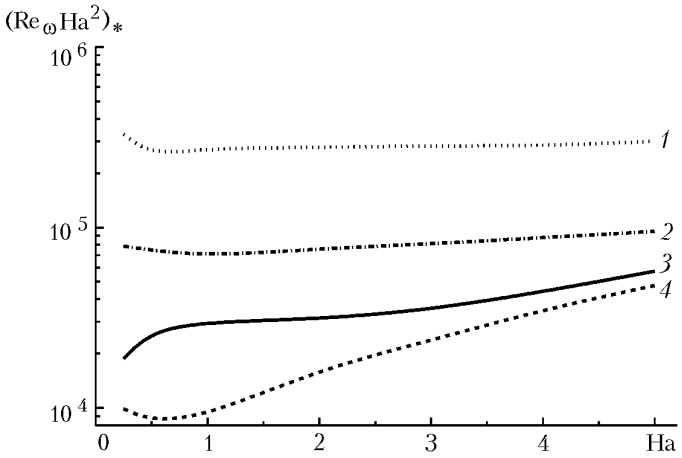

Fig. 7. Stability of the flow induced by the rotating magnetic field in a cylinder with a free side surface versus the Hartmann number: 1) L/R = 0.5; 2) 1; 3) 2; 4) 3. Pr = 0.018 (Ge (Ga)).

The boundary of the transition to the oscillating convection regime at an interaction of the RMF with thermal gravitational and thermocapillary convection is shown in Fig. 6a and b, respectively. The zone of laminar flows lies below the curves given in these figures. The boundary of the transition to the oscillating regime of pure gravitational convection is given in Fig. 6a by vertical dotted lines for a Grashof number equal to $1.2 \cdot 10^6$ when the gravitational acceleration is directed upward from the crystallization boundary and $9.5 \cdot 10^8$ in the case of the opposite direction of this vector. The rotating magnetic field does not promote an increase in the stability of thermal gravitational convection in all the regimes considered. It should be noted that if the flow conditions are oscillating, then oscillations continue at any intensity of the RMF. For thermocapillary convection, the situation is different. This is confirmed by the data given in Fig. 6b. The complicated and ambiguous dependence of the boundary of the transition to the oscillating regime at a combination of thermocapillary convection with an RMF is explained by the change in the velocity gradient at the boundary (r = 1) and ends with increasing Marangoni number and Ha^2Re_ω parameter. The point for Ma = 2430 and $Ha^2Re_\omega = 2 \cdot 10^3$ lies below the flow stability curve. The effect of the Hartmann number on the boundary of the transition to the oscillating convection regime is relatively small, which is clearly seen from Fig. 7.

In a real three-dimensional flow, oscillations arise earlier than in a two-dimensional axially symmetric flow because of the appearance of a small azimuthal velocity. In such a situation, the RMF, creating a large azimuthal velocity, should lead to the elimination of this reason for hydrodynamic instability, which has been corroborated by experiments [10]. They have also shown that the oscillation spectrum has no magnetic-field rotation frequency. This confirms the validity of the method of averaging over the magnetic-field rotation frequency used in the present work.

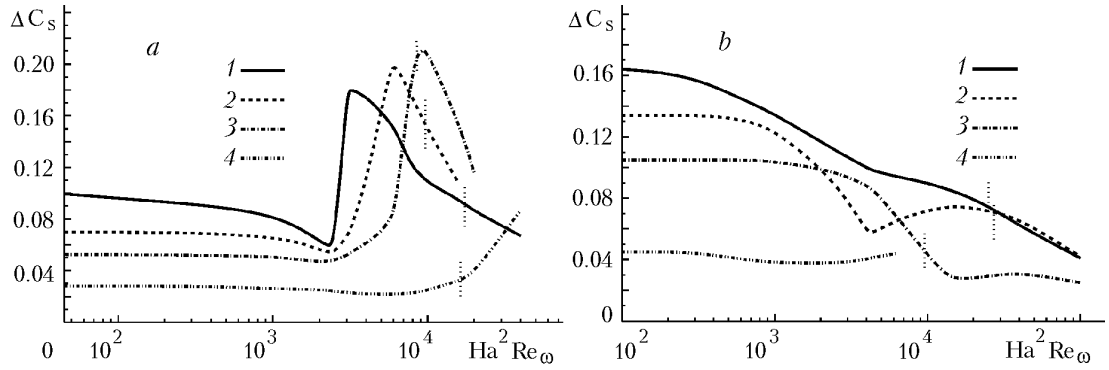

Fig. 8. Effect of the rotating magnetic field on the radial macrosegregation of antimony in the silicon crystal grown on the ground by the Bridgman method. Ha = 0.158; Pr = 0.023, Sc = 5, k = 0.023, Re_{cr} = 0.2. Vector g is directed to the crystallization boundary — a [1) Gr = $1.6 \cdot 10^5$; 2) $4 \cdot 10^5$; 3) $1 \cdot 10^6$; 4) $1 \cdot 10^7$] and from it — b [1) Gr = $3 \cdot 10^4$; 2) $1.6 \cdot 10^5$; 3) $1 \cdot 10^6$; 4) $1 \cdot 10^7$].

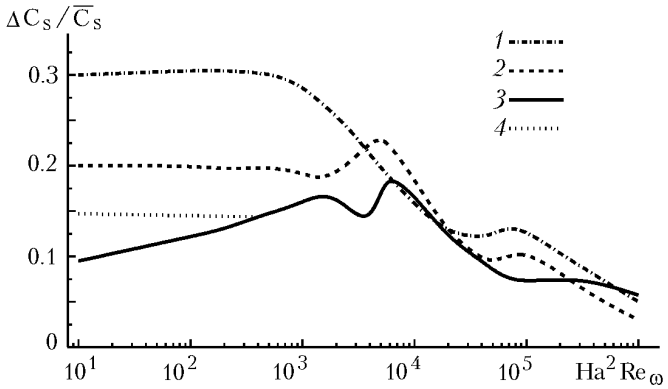

Fig. 9. Effect of the rotating magnetic field on the relative radial macrosegregation of gallium in the germanium crystal grown in zero gravity by the floating zone method: 1) Ma = 130 and Ha = 2; 2) 680 and 2; 3) 2430 and 0.5, 1, and 2; 4) 2430 and 2. Re_ω is variable, Sc = 10, k = 0.023, Re_{cr} = 0.2.

2.2. Effect of the RMF on the Impurity Transfer in the Liquid. Once the boundary of the transition to the oscillating convection regime has been determined and crystal growth occurs in the laminar-flow conditions, which excludes impurity microsegregation (impurity banding) due to the convection, we also formulate the problem of decreasing the impurity macrosegregation, in particular, the radius inhomogeneity of the crystal. To this end, it is important not only to control the mean convection intensity of the liquid, but also to perform a finer control of the relation between the radial and axial velocities in the region adjoining the crystallization boundary. A rotating magnetic field can be used for this purpose.

The dependence of the radial inhomogeneity of the impurity distribution in the melt at the crystallization boundary $\Delta C_s = C_{s,max} - C_{s,min}$ on the thermal gravitational convection intensity is given in Fig. 8 for two mutually opposite directions of gravitational acceleration g. The radial impurity distribution is highly sensitive to the relation between the radial and axial velocities in the vicinity of the crystallization boundary. The interaction of flows so widely differing in structure (see Fig. 5) at their different intensities gives a strongly varying relation between the velocity components in this region, which leads to unexpected results (see Fig. 8a). The example of the silicon crystal with an antimony impurity grown by the Bridgman method on the ground shows that, instead of a decrease, one can obtain, in specific regimes, a sharp increase in the impurity macrosegregation. Such an unusual and strong effect of the RMF revealed in the present study should be taken into account in using it in the ground technology.

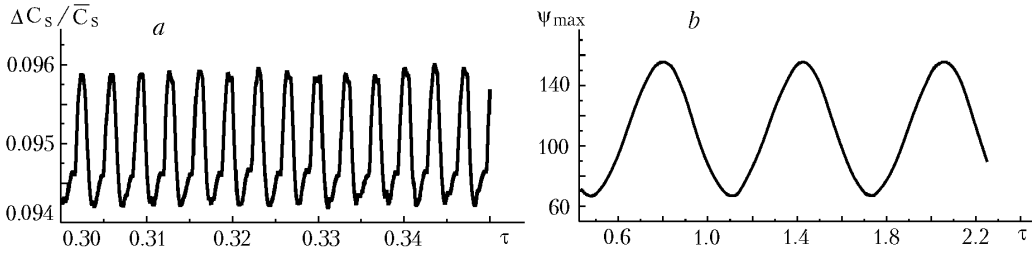

Fig. 10. Oscillations of parameters in the liquid at a combination of thermocapillary convection with a rotating magnetic field: Ma = 1280, Pr = 0.018, Sc = 10, k = 0.023, Re_{cr} = 0.2, Ha = 2, $Re_\omega = 1.5 \cdot 10^4$, a = 0.8, b = 0.3, L/R = 2 (a); Ma = 1150, Pr = 0.018, Ha = 0.3, $Re_\omega = 9.5 \cdot 10^4$, a = 0.8, b = 0.3, and L/R = 3 (b).

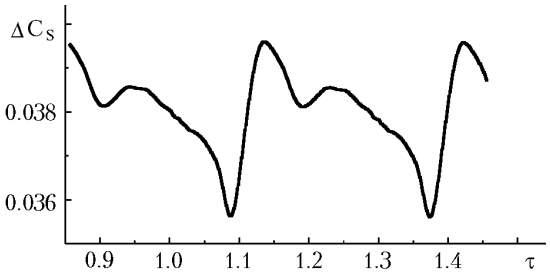

Fig. 11. Oscillation of the radial impurity segregation under the action of a rotating magnetic field for the Si(Sb) crystal grown on the ground by the Bridgman method (vector g is directed to the crystallization boundary). Gr = 10^7, Pr = 0.023, Ha = 0.158, $Re_\omega = 5 \cdot 10^5$, Sc = 5, k = 0.023, Re_{cr} = 0.2, a = 0.8, b = 0.3, and L/R = 3.

As is known, the oscillating convection regime is one of the main reasons for the appearance of impurity bands in the crystal (impurity microsegregation). Therefore, in choosing the RMF parameters, one should know the position of the boundary of the transition to the oscillating regime (Fig. 6) to avoid this convection regime.

For crystal growth by the floating-zone method in zero gravity, a real possibility of positively influencing the impurity macrosegregation by using an RMF exists. In so doing, the dependences of the relative radial inhomogeneity of the impurity distribution on the Ha^2Re_ω parameter given in Fig. 9 for germanium with a gallium impurity show that there is a possibility of decreasing the radial impurity macrosegregation. However, to achieve this result, a preliminary study on the optimization of the magnetic-field parameters is required. It is also necessary to take into account the effect of the RMF on the boundary of the transition to oscillations for mixed convection (Fig. 6b).

As mentioned above (Fig. 6), the rotating magnetic field does not always stabilize the flow. Even a laminar flow without a magnetic field, in using an RMF with wrongly chosen parameters, can lose its hydrodynamic stability, and oscillations of all parameters will arise. This is clearly shown by the data given in Fig. 10. In this case, low-frequency oscillations leading to the appearance of wide impurity bands may arise (Fig. 11). Specific oscillations of the type of beats appear sometimes at a combination of three types of convection: thermal gravitational, thermocapillary, and secondary flow due to the RMF in a cylinder with a free side surface (Fig. 12). Such regimes are possible in the process of crystal growth on the ground by the floating-zone method with an RMF. In the presence of low-frequency oscillations of the type of beats, in the crystal wide impurity bands are formed in which thinner layers with a varying impurity concentration are situated. Specific oscillations of parameters in the liquid may also arise under the action of the RMF alone, as shown in Fig. 13.

CONCLUSIONS

The numerical investigation of the effects of an RMF under different conditions of crystal growth has shown that by using such fields, it is possible to effectively control the melt flow and impurity transfer. However, such an

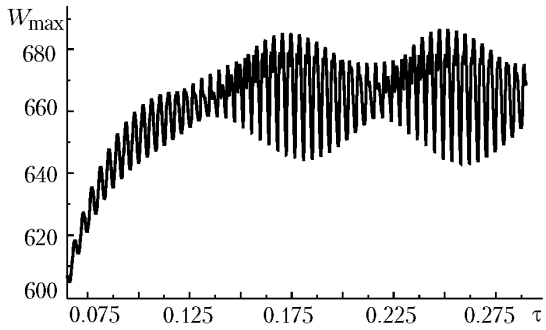

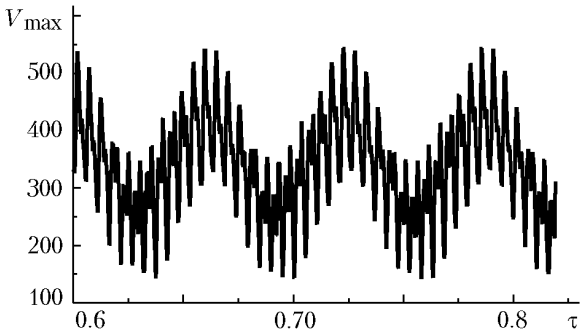

Fig. 12. Oscillation of the azimuthal velocity maximum at a combination of thermocapillary and thermal gravitational velocity with a rotating magnetic field. Gr = $3.4 \cdot 10^4$, Ma = 1700, Pr = 0.023, Ha = 0.882, and $\mathrm{Re}_\omega = 4.4 \cdot 10^4$.

Fig. 13. Oscillation of the maximum axial velocity in a rotating liquid with a free side surface. Pr = 0.023, Ha = 1, $\mathrm{Re}_\omega = 5.5 \cdot 10^4$, and $L/R = 2$.

action on the process of crystal growth can lead to both positive and negative results. The floating-zone method is most promising for obtaining homogeneous monocrystals with the use of an RMF in microgravity. In so doing, to obtain crystals with improved characteristics of the micro- and macrohomogeneities, a very exact determination of the optimal parameters of the magnetic field is required. Mathematical modeling and numerical calculations can help in choosing a zone of such optimal parameters. It may also be supposed that the revealed regimes of specific oscillations can be used in the technology of obtaining materials in which the generation of bands with a variation of the physical properties is required.

RMF-excited flows belong to the class of flows in a rotating liquid. Not only are they widely used in technological processes, but they have also long been a subject of investigation in geophysical applications. Atmospheric vortices, tornados, long-lived vortices in the ocean — this is an incomplete list of such problems. However, the potentialities of such a physical modeling are rather limited. Mathematical modeling is a very flexible tool for solving such problems, since one can arbitrarily give any physical properties of the medium and boundary conditions. We have used our programs for numerical study of the stability of vortex flows in homogeneous and stratified liquids for investigating certain geophysical problems [17]. In particular, it has been shown that the formation of specific low-frequency oscillations combined with high-frequency oscillations is possible (Fig. 13).

This work was supported by the INTAS, project INTAS-2000-0617.

NOTATION

a, *b*, dimensionless coefficients in (10); **B** and *B*, magnetic induction vector and modulus, T; *c*, impurity concentration in the liquid, kg/m^3; $C = c/c_0$, dimensionless impurity concentration; *D*, diffusion coefficient of impurity in the liquid, m^2/sec; **E** and *E*, electric field strength vector and modulus, V/m; *F*, Lorentz force per unit volume of liquid, in (6) and (7), N/m^3; *g*, gravitational acceleration, m/sec^2; $\mathrm{Gr} = g\beta_T \Delta T R^3 \nu^{-2}$, Grashof number; $\mathrm{Ha} = BR(\lambda/\rho\nu)^{1/2}$, Hartmann number; **j**, electric current density vector; A/m^2; *k*, dimensionless equilibrium impurity distribution coefficient; *L*, liquid length in a cylindrical space, m; $\mathrm{Ma} = -(\partial\sigma/\partial T)\Delta T R(\rho\nu\chi)^{-1}$, Marangoni number; *p*, pressure, Pa; $\mathrm{Pr} = \nu\chi^{-1}$, Prandtl number; *r*, *z*, and φ, cylindrical coordinates, m and rad; *R*, cylindrical liquid zone radius, m; $\mathrm{Re}_x = xR\nu^{-1}$, Reynolds number for velocity components ($x = u, v, w$); Re_m, magnetic Reynolds number; $\mathrm{Re}_{cr} = v_{cr}R\nu^{-1}$, dimensionless crystallization rate; $\mathrm{Re}_\omega = \omega R\nu^{-2}$, dimensionless angular rotation velocity of the magnetic field; $\mathrm{Sc} = \nu D^{-1}$, Schmidt number; *t*, time, sec; *T*, temperature, K; *U*, *V*, *W*, characteristic flow velocities; *u*, *v*, *w*, components of the velocity vector **V** on the *r*, *z*, φ axes, respectively, m/sec; β_T, temperature expansion coefficient of the liquid, K^{-1}; ΔC_s, radial concentration difference; $\Delta C_s/C_s$, relative radial impurity concentration difference; $\Delta T = T_{max} - T_{min}$, characteristic temperature differences in the system, K; $\theta = (T - T_{min})/\Delta T$, dimensionless temperature; λ, specific conductivity of the liquid, 1/(Ω·m); $\mu_0 = 4\pi \cdot 10^{-7}$, magnetic constant, H/A^2; ν, kinematic viscosity of the liquid, m^2/sec; ρ, liquid density, kg/m; σ, surface tension coefficient of the liquid, H/m; χ, thermal diffusivity of the liquid, m^2/sec; τ, dimensionless time; ψ, dimensionless stream function; ω, circular rotation frequency of the magnetic

field, sec^{-1}. Subscripts: cr, crystallization; max, maximum; min, minimum; s, at the crystallization boundary; *x*, points to the velocity vector projection on the axis for the Reynolds number; ω, magnetic field rotation; *, boundary of the transition to oscillations; 0, initial value; overscribed bar, parameter averaging; m, magnetic.

REFERENCES

1. P. A. Davidson, Estimation of turbulence/velocities induced by magnetic stirring during continuous castings, *Mater. Sci. Technol.*, **1**, No. 11, 994–999 (1985).
2. V. I. Doronin, V. V. Dremov, and A. B. Kapusta, Measurement of the characteristics of the mercury MHD flow in a closed cylindrical vessel, *Magn. Gidrodin.*, No. 3, 138–140 (1973).
3. P. A. Davidson and J. C. R. Hunt, Swirling recirculating flow in a liquid-metal column generated by a rotating magnetic field, *J. Fluid Mech.*, **185**, 67–106 (1987).
4. L. P. Gorbachev, N. V. Nikitin, and A. L. Ustinov, MHD rotation of a conducting liquid in a cylindrical vessel of finite size, *Magn. Gidrodin.*, No. 4, 32–42 (1974).
5. L. A. Gorbunov and V. L. Kolevzon, Conducting liquid flow in a rotating magnetic field, *Magn. Gidrodin.*, No. 4, 69–74 (1992).
6. Yu. M. Gelfgat, M. Z. Sorkin, J. Priede, and O. Mozgirs, On the possibility of heat and mass transfer and interface shape control by electromagnetic effect on melt during unidirectional solidification, in: *Proc. of the First Int. Symp. on Hydromechanics and Heat/Mass Transfer in Microgravity*, Perm–Moscow, 1991, Gordon and Breach, Amsterdam (1992), pp. 429–434.
7. A. S. Senchenkov, I. V. Friazinov, and M. P. Zabelina, Mathematical modeling of convection during crystal growth by the THM, Ibid, 455–459.
8. M. P. Marchenko, A. S. Senchenkov, and I. V. Fryazinov, Mathematical modeling of the process of crystal growth from the solution-melt by the moving-heater method, *Mat. Model.*, **4**, No. 5, 67–79 (1992).
9. M. Salk, C. Eiche, M. Friederle, W. Joergen, K. W. Benz, A. S. Senchenkov, and A. V. Egorov, The influence of different materials transport regimes on the radiation detector properties of CdTe:Cl, $C_{0.9}Z_{0.1}$Te:Cl, and $CdTe_{0.9}Se_{0.1}$:Cl, in: *Abstr. of Papers presented at Ninth Eur. Symp. "Gravity-Dependent Phenomena in Physical Sciences*," 2–5 May 1995, Berlin, Germany (1995), pp. 253–254.
10. P. Dold, A. Croll, M. Lichtensteiger, Th. Kaiser, and K. W. Benz, Floating zone growth of silicon in magnetic fields: IV. Rotating magnetic fields, *J. Cryst. Growth*, **231**, Nos. 1–2, 95–106 (2001).
11. A. I. Feonychev and G. A. Dolgikh, Effects of constant and time-variable accelerations in crystal growth by the method of directed crystallization on board space vehicles, *Kosm. Issled.*, **39**, No. 4, 390–399 (2001).
12. A. I. Feonychev and G. A. Dolgikh, Effect of magnetic field on crystal growth process under action of gravity or capillary force, in: *Abstr. of Papers presented at Ninth Eur. Symp. "Gravity-Dependent Phenomena in Physical Sciences*," 2–5 May 1995, Berlin, Germany (1995), p. 246.
13. A. I. Feonychev, Comparative analysis of thermocapillary convection in one- and two-layer systems. Problem of oscillatory convection, *Adv. Space Res.*, **16**, No. 7, 59–65 (1995).
14. A. I. Feonychev and I. S. Kalachinskaya, Effect of variable accelerations on crystal growth by the floating-zone method on board space vehicles, *Kosm. Issled.*, **39**, No. 4, 400–406 (2001).
15. A. I. Feonychev and N. V. Bondareva, Influence of a rotating magnetic field on the transition to the oscillating convection regime and on crystal growth by the floating-zone method in zero gravity, in: *Ext. Abstr. of Papers presented at Winter (13th) School on Continuum Mechanics* [in Russian], Perm' (2003), p. 55.
16. L. D. Landau and E. M. Lifshits, in: *Theoretical Physics* [in Russian], Vol. 7, Nauka, Moscow (1982), pp. 319–320.
17. A. I. Feonychev and N. V. Bondareva, Laminar and turbulent flows in homogeneous and stratified rotating field, in: *Abstr. of Papers presented at 27th General Assembly of the Eur. Geophys. Soc.*, 21–26 April (2001), Nice, France. EGS02–A–01226.